SIMS ANALYSIS OF WATER ABUNDANCE IN NOMINALLY ANHYDROUS MINERALS IN LUNAR BASALTS. Y. Liu[1], J. L. Mosenfelder[2], Y. Guan[2], G. R. Rossman[2], J. M. Eiler[2], and L. A. Taylor[1], [1]Planetary Geosciences Institute, Department of Earth & Planetary Sciences, University of Tennessee, Knoxville, TN 37996, (yangl@utk.edu), [2]Division of Geological and Planetary Sciences, California Institute of Technology, Pasadena, CA 91125.

Introduction: Indications of high abundances of "water" (broadly referring to both OH and H_2O) in the lunar mantle, possibly ranging up to the amount estimated for Earth's upper mantle, have been provided through analyses of lunar volcanic glasses [1], mesostasis apatite in rocks [2-5], and melt inclusions in olivines erupted with volcanic glasses [6]. The amount of lunar mantle water was estimated to range from 64 ppb to 750 ppm [1-6]. This naturally leads to numerous questions, such as: Where would the water be in lunar mantle? What is the Moon's water budget? Bell and Rossman [7] demonstrated that water in Earth's mantle is largely stored as hydroxyl (OH) in nominally anhydrous minerals (NAMs), the amount of which is comparable to the current ocean mass. Could this be the case for the Moon?

It is debated, however, whether the Moon contains high abundances of water. Sharp et al. [8] argued that high $^{37}Cl/^{35}Cl$ ratios characteristic of some lunar igneous materials require H_2O-poor lunar magmas and thus supported the previous concept of a "dry" interior of the Moon. The model of magma-ocean solidification by Elkins-Tanton and Grove [9] obtained 0.05-4.7 wt% H_2O in the final 2 vol% of magma ocean (urKREEP) for initial water contents of 10-1000 ppm. On the basis that H_2O contents in a KREEP-rich clast from soil 15404 is lower than non-KREEP mare basalts [4], Elkins-Tanton and Grove [9] argued that mantle source regions for volcanic glasses and mare basalts should have <10 ppm H_2O.

The controversy between a wet versus dry Moon can be explained by heterogeneous distribution of water in lunar mantle [4, 10-11]. However, the debate can also be largely attributed to the fact that many thermodynamic data (e.g., partition coefficients, solubility, diffusivity) have not been determined for the highly reduced conditions on the Moon [3, 12]. As a result, H may exist as H_2, H_2O, and C-H in vapor and melt, and the rapid diffusion and low solubility of H_2 could play an important role in altering the total abundance of hydrogen in lunar samples [12]. To date, all measurements have exclusively determined H. One line of evidence for the dry-Moon theory was the low H_2O contents in KREEP-rich rocks [4, 9-10]. However, none of the KREEP-rich rocks in the Apollo collections represent the final liquid of the magma ocean (urKREEP). The KREEP-rich rocks in [4, 11] are small clasts from soils and with questionable shock histories and origins.

Here, we report our preliminary results OH analysis of NAMs near and associated with the late-stage KREEP-rich mesostases in lunar basalts, in order to gain insights into H partitioning between glass/NAMs under its natural reduced conditions.

Methods: The description of mesostasis in lunar rocks is often inadequate and inconsistent in the literature. Mesostasis in each basalt is rather isolated, as they are interstitial melts after >95% crystallization. This can result in a rather large variation in mineralogy (Fig. 1). In order to estimate the total budget of water in a given sample, the total amount of mesostasis and the mineralogy of each mesostasis must be determined. Using a Cameca SX100 EMP at the University of Tennessee, X-ray maps of Si, Ti, Ca, Fe, K, F, P, and Ba were obtained on one thin section of Apollo 12 basalt 12063 (,18) with a total area of ~90 mm^2.

One chip each from Apollo 12 basalt 12063,321, Apollo 12 basalt 12056, 18, and Apollo 17 basalt 74255,185 were polished and analyzed by EMP. Together with these chips, standards of dry and wet olivines (0, 16 and 54 ppm H_2O, [14]) and one clinopyroxene were pressed into indium for analyses using a Cameca ims-7f GEO ion probe (SIMS) at Caltech.

SIMS analytical procedures are similar to those in Mosenfelder et al. [14]. To minimize H (and thus $^{16}O^1H$) backgrounds, the instrument was baked for 24 h prior to the session, and samples were kept in the sample storage chamber (at 10^{-9} torr) for ~72 h prior to analysis. The $^{16}O^1H$ backgrounds for standards and samples were assessed periodically by analyzing a dry olivine, GRR1017 (<<1 ppm H_2O). We used a Cs^+ primary beam with a current of 5 nA and an impact energy of 10 keV to sputter the sample and produce negative secondary ions. Calibration for olivine was conducted on a separate mount using standards with 0-220 ppm H_2O [14]. Calibration for pyroxenes was performed on 11 orthopyroxenes and 13 clinopyroxenes with H_2O contents ranging from 0 to 515 ppm. Measurements on the secondary standards mounted together with the Apollo chips show negligible drift in the calibrations.

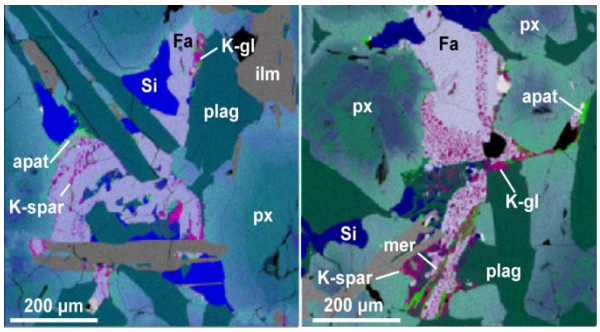

Fig. 1. *Combined X-ray maps of two mesostases in 12063, 18. Abbreviations are: apat, apatite; Fa, fayalite; ilm, ilmenite; k-gl, K-rich glass; K-spar, K-rich feldspar; mer, merrillite; plag, plagioclases; px, pyroxene; Si: tridymite.*

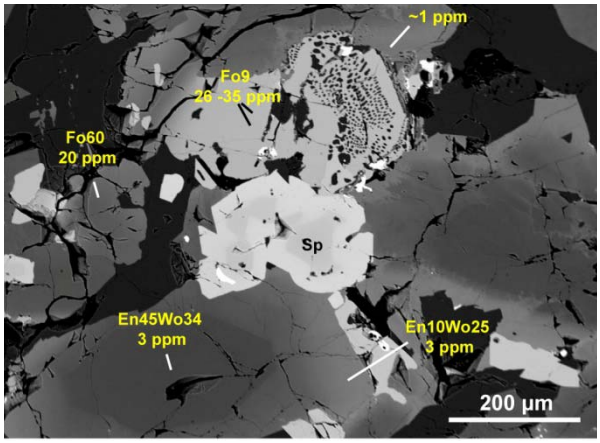

Fig. 2. *BSE map of the area in rock chip of 12063,321 analyzed by SIMS. Spinel (Sp) shows enrichment of Ti toward the rim.*

SIMS analyses were placed near the EMP analysis spots. The areas of interest were examined carefully using ion imaging to avoid C and H hotspots in cracks. Following ~4 min sputtering, olivine and pyroxene in lunar rocks were measured for multiple cycles through the mass sequence of ^{12}C, $^{16}O^{1}H$, ^{18}O, ^{19}F, and ^{30}Si. A mass resolving power of 5500 was used to separate $^{16}O^{1}H$ from ^{17}O.

Results:

Abundances of mesostasis. X-ray maps were collected for the whole section at low magnification and then for individual mesostasis at high magnification. Mesostasis was defined as the late-stage, fine-grained areas containing silica-rich phases (tridymite and glass), fayalite, K-rich glass, K-spar, and phosphates. Mineral abundances in these mesostases were measured on high-magnification X-ray maps using ImageJ. These X-ray maps were then scaled to generate the abundances in the whole section. The total abundance of mesostasis in 12063, 18 is ~4.8 vol% of the sample, similar to the literature data [15]. Mineralogy of mesostasis varies greatly among different mesostases, even within the same thin-section (Fig.1).

SIMS results. The OH contents in olivine and pyroxenes were calculated on the background corrected $^{16}O^{1}H/^{30}Si$ values. Because of the numerous cracks in the sample, Mg-rich olivine and pyroxene in each rock chip were deemed to be H-free owing to its low-P formation and were used to check for contamination.

For Apollo 12 basalt 12063, mesostasis olivine (Fo_9) contains higher OH (26-35 ppm H_2O) than the phenocrystic olivine (Fo_{60}, 20 ppm H_2O) (Fig. 2). For a phenocrystic pyroxene in 12063, the Mg-rich interior ($En_{45}Wo_{34}$) shows similar OH content (3 ppm) to the Fe-rich rim (Fig. 2). Phenocrystic pyroxenes in Apollo 12 basalt 12056 ($En_{15}Wo_{25}$- $En_{58}Wo_9$) have no detectable OH. Phenocrystic pyroxenes ($En_{43\text{-}45}Wo_{42\text{-}39}$) in Apollo 17 basalt 74255 contain 10-20 ppm H_2O. A phenocrystic olivine (Fo_{66}) in 74255 shows ~5 ppm H_2O.

Discussion: Results of detectable OH in Fe-rich NAMs are encouraging. It is expected that Fe-rich pyroxenes will display higher OH values than Fe-rich olivines. However, the observation indicates Fe-rich pyroxenes contain lower OH than Fe-rich olivines. The possible explanation is that these pyroxenes formed earlier than the late-stage fayalite, and thus may have equilibrated with melt of lower OH. Our results represent our first attempt to constrain the OH contents in late-stage NAMs. More studies are underway to refine the results and sample preparation techniques.

References: [1] Saal A. E. *et al.* (2008) *Nature, 454*, 192-196. [2] Liu Y. et al. (2010) *LPSC 41st*, #2647. [3] Boyce J. W. *et al.* (2010) *Nature, 466*, 466-469. [4] McCubbin F. M. *et al.* (2010) *PNAS, 107*, 11223-11228. [5] Greenwood J. P. *et al.* (2011) *Nature Geosci, 4*, 79-82. [6] Hauri E. H. *et al.* (2011) *Science, 333*, 213-215. [7] Bell D. R. and Rossman G. R. (1992) *Science, 255*, 1391-1397. [8] Sharp Z. D. *et al.* (2010) *Science, 329*, 1050-1053. [9] Elkins-Tanton L. T. and Grove, T L. (2011) *EPSL, 304*, 326-336. [10] Anand M. (2011) *Earth, Moon, & Planets, 107*, 65-73. [11] McCubbin F. M. *et al.* (2011) *GCA, 75*, 5073-5093. [12] Zhang Y. (2011) *LPSC 42nd*, 1957. [13] Taylor L.A. (2011) In: *The Moon: the first billion years of crystal formation*. [14] Mosenfelder J. L. *et al.* (2011) *Am. Min.*, 96, 1725-1741. [15] Meyer C (2011) *Lunar Sample Compendium. http://curator.jsc.nasa.gov/lunar/compendium.cfm.*